

Additional Disruption of the CIC-2 Cl⁻ Channel Does Not Exacerbate the Cystic Fibrosis Phenotype of Cystic Fibrosis Transmembrane Conductance Regulator Mouse Models*

Received for publication, September 5, 2003, and in revised form, February 25, 2004
Published, JBC Papers in Press, March 7, 2004, DOI 10.1074/jbc.M309899200

Anselm A. Zdebik[‡], John E. Cuffe[§], Marko Bertog^{§¶}, Christoph Korbmacher^{§¶},
and Thomas J. Jentsch^{‡||}

From the [‡]Zentrum für Molekulare Neurobiologie (ZMNH), Falkenried 94, D-20246 Hamburg, Germany and the [§]University Laboratory of Physiology, Oxford University, Parks Road, Oxford OX1 3PT, United Kingdom

Cystic fibrosis is a fatal inherited disease that is caused by mutations in the gene encoding a cAMP-activated chloride channel, the cystic fibrosis transmembrane conductance regulator (CFTR). It has been suggested that the cystic fibrosis phenotype might be modulated by the presence of other Cl⁻ channels that are co-expressed with CFTR in some epithelial cells. Because the broadly expressed plasma membrane Cl⁻ channel, CIC-2, is present in the tissues whose function is compromised in cystic fibrosis, we generated mice with a disruption of both Cl⁻ channel genes. No morphological changes in their intestine, lung, or pancreas, tissues affected by cystic fibrosis, were observed in these mice. The mortality was not increased over that observed with a complete lack of functional CFTR. Surprisingly, mice expressing mutant CFTR (deletion of phenylalanine 508), survived longer when CIC-2 was disrupted additionally. Currents across colonic epithelia were investigated in Ussing chamber experiments. The disruption of CIC-2, in addition to CFTR, did not decrease Cl⁻ secretion. Colon expressing wild-type CFTR even secreted more Cl⁻ when CIC-2 was disrupted, although CFTR transcript levels were unchanged. It is concluded that CIC-2 is unlikely to be a candidate rescue channel in cystic fibrosis. Our data are consistent with a model in which CIC-2 is located in the basolateral membrane.

Cystic fibrosis (CF)¹ is a severe autosomal recessive disease that is associated with pulmonary, pancreatic, and intestinal symptoms. Most patients eventually die in adulthood because of the pulmonary phenotype. In the lung and trachea, very viscous tracheal mucus results in reduced lung clearance and accompanying recurrent bacterial infections. In addition, the pancreas often undergoes cystic and fibrotic changes with aging, resulting in pancreatic insufficiency in some, but not all, patients. Further symptoms include male infertility due to the

congenital absence of vas deferens and, in some cases, an intestinal occlusion due to thick feces (meconium ileus) and biliary cirrhosis.

Cystic fibrosis is caused by mutations in the gene encoding the cystic fibrosis transmembrane conductance regulator (CFTR) (1), the only member of the large ABC transporter family that is known to function as a cAMP-activated chloride channel. The most common CFTR mutation in Caucasians is $\Delta F508$, which deletes a phenylalanine (Phe-508) in-frame. More than one thousand other mutations, many of them leading to a complete loss of function, are known. CFTR mediates chloride transport in the apical membranes of many epithelia. In addition, CFTR was suggested to have several other functions, including the regulation of various transport proteins such as the epithelial Na⁺ channel ENaC and certain other Cl⁻ channels (2–4). If the pathological changes in cystic fibrosis were predominantly due to defective chloride transport, the pharmacological activation of other Cl⁻ channels present in the same membranes would potentially prove beneficial in patients.

Several CFTR mouse models have been generated. They include complete disruptions of the CFTR gene (as in the *Cftr*^{unc/unc} mouse (5), called *Cftr*^{-/-} from here on) and mice that carry CFTR point mutations analogous to those found in patients (like the *Cftr*^{kth/kth} mouse as a model for the human $\Delta F508$ mutation (6), called *Cftr* ^{$\Delta F/\Delta F$} from here on). These mice, however, failed to show obvious pulmonary and pancreatic phenotypes, but rather exhibited intestinal occlusion (ileus). Without a laxative diet these mice rarely survive beyond the age of 30 days. But even when fed an osmotic laxative, no clear pulmonary and pancreatic phenotypes developed at older ages. The discrepancy between human and mouse pathology may be explained, for example, by differences in airway anatomy or by the expression of other Cl⁻ channels that may compensate for the loss of CFTR in mice. Among the several putative modifier genes that co-determine the severity of CF, there may be genes encoding other Cl⁻ channels (7, 8).

The CLC gene family encodes nine Cl⁻ channels in mammals (9). Many other Cl⁻ channels, probably including Ca²⁺-activated Cl⁻ channels, have not yet been identified at the molecular level. Human mutations in several CLC channel genes underlie diseases as diverse as myotonia (10), the kidney diseases Bartter syndrome (11) and Dent's disease (12), osteopetrosis (13), and possibly a form of epilepsy (14). Only four CLC channels, *i.e.* CIC-1, CIC-2, CIC-Ka, and CIC-Kb, reside predominantly in the plasma membrane. CIC-2 is nearly ubiquitously expressed in epithelia and non-epithelial tissues (15). CIC-1 is muscle-specific (16), and CIC-K expression is probably limited to certain renal cells and the stria vascularis (17).

* This work was supported by a Wellcome Trust grant (to C. K.), the Ernst Jung Preis für Medizin, and a grant from the Cystic Fibrosis Foundation (United States) (to T. J. J.). The costs of publication of this article were defrayed in part by the payment of page charges. This article must therefore be hereby marked "advertisement" in accordance with 18 U.S.C. Section 1734 solely to indicate this fact.

[¶] Present address: Inst. für Zelluläre und Molekulare Physiologie, Waldstr. 6, D-91054 Erlangen, Germany.

^{||} To whom correspondence should be addressed. Tel.: 49-40-42803-4741; Fax: 49-40-42803-4839; E-mail: Jentsch@zmnh.uni-hamburg.de.

¹ The abbreviations used are: CF, cystic fibrosis; CFTR, CF transmembrane conductance regulator; CLC, a gene family of chloride channels originally identified by the cloning of the *Torpedo* channel CIC-0; WT, wild type; DPC, diphenylcarboxylate; ENaC, epithelial sodium channel.

Immunocytochemical studies have suggested that CIC-2 is expressed in the apical membranes of lung and intestinal epithelia (18, 19), where it may transport Cl^- in a pathway that is independent of and parallel to CFTR. Thus, CIC-2 appears to be a prime candidate for an alternative pathway for Cl^- secretion in CF (20–22).

CIC-2 is activated by hyperpolarization, cell swelling, and acidic extracellular pH (15, 20, 23). Many physiological functions have been postulated for CIC-2 (9), but blindness and male infertility were, surprisingly, the only phenotypes noted in CIC-2 knock-out mouse models (24, 25). An impaired transepithelial transport across the retinal pigment epithelium and Sertoli cells was hypothesized as the mechanism underlying the retinal and testicular degeneration, respectively (24). Indeed, Ussing chamber experiments revealed that transepithelial voltage and resistance were reduced in the pigment epithelium of *Cln2*^{-/-} mice (24).

If CIC-2 transports chloride across the same cell membranes as CFTR, then a disruption of both channels should lead to a more severe phenotype in the respective tissues. This may then also include the lung and the pancreas, tissues that are affected in CF patients but not in CFTR mouse models. We therefore produced mice in which both genes are disrupted. In addition to histomorphological analysis, we performed Ussing chamber experiments on colon and trachea, tissues that are affected in CF.

EXPERIMENTAL PROCEDURES

Mice—CIC-2 knock-out mice, described previously (24) and backcrossed for seven generations into C57Bl6, were mated with heterozygous CFTR ΔF508 mice (6) (CFTR^{hth}, called *Cfr* ^{$\Delta\text{F}/\Delta\text{F}$}) and CFTR S489X mice (5) (CFTR^{unc}, called *Cfr*^{-/-}) (26) (both in C57Bl6 background) obtained from Jackson Laboratories. Both types of mutations lead to a severe phenotype in humans. The resulting offspring were again mated. Genotypes were determined by touch-down PCR (3 + 37 cycles) on tail DNA, using the following: C2wtF1 (5'-GGGTACAGAGTAGGAACACTTTG-3'), C2wtR1 (5'-AGGTTAGCCCAATGACCTTAGC-3'), and PGK (5'-CTAAAGCGCATGCTCCAGACTGCC-3') for genotyping the CIC-2 locus; primers IMR0269/0270/0271 (5'-TTCAAGCCCAAGCTTTCGCGA-3', 5'-CTCCCTTCTTCTAGTACAACCG-3', and 5'-CATCTTGATAGAGCCACGGTGC-3', respectively) for *Cfr* ^{$\Delta\text{F}/\Delta\text{F}$} ; and primers IMR-1125/1126/1127 (5'-GAGAACTGGAAGCTTCAGAGG-3', 5'-TCCATCTTGTTCATGGCC-3', and 5'-TCCATGTAGTGGTGTGAACG-3', respectively) for *Cfr*^{-/-} (as described by Jackson Laboratories). Mice were fed a normal mouse diet (ssniff, Soest, Germany), but water was replaced by an osmotic laxative (26) containing 25 mM NaCl, 40 mM Na₂SO₄, 20 mM NaHCO₃, 18 mM polyethylene glycol 3000, and 10 mM KCl. Mice were housed under virtually standard pathogen-free (SPF) conditions. For some experiments, mice in which only CIC-2 was disrupted were fed a low Na⁺ diet (100 mg NaCl/kg) for 2 weeks prior to the experiment.

Ussing Chamber Measurements—In one series of experiments (Fig. 4), a custom-made, temperature-controlled (37°C), perfusable Ussing chamber with a tissue area of 10 mm² (kindly provided by Dr. Markus Bleich) was used. Solutions were based on bicarbonate-free Ringer's solution (145 mM NaCl, 0.4 mM KH₂PO₄, 1.6 mM K₂HPO₄, 5 mM glucose, 1 mM MgCl₂, and 1.3 mM calcium gluconate₂). The colon of 1–3 months old mice was stripped of muscle and connective tissue layers (distal colon, only the most distal 3 cm *ab ano* were used). Any nerve plexus activity in the partially remaining myenteric plexus was blocked by the basolateral addition of tetrodotoxin acetate (1 μM), local PGE production was inhibited by the addition of indomethacin (10 μM , predissolved in methanol), and secretion was induced by the basolateral addition of forskolin (Tocris)(10 μM) to the luminal perfusate. Amiloride (Sigma) and bumetanide (ICN) were predissolved in Me₂SO as a 1 M stock solution and diluted to 10 and 100 μM , respectively. A custom-made differential amplifier (U. Froebe, University of Freiburg, Germany) equipped with a current pulse generator was used to measure the transepithelial potential (V_{te}) in the open circuit mode (at $I = 0$). In regular intervals, a current of 1 μA was injected, and the transepithelial resistance (R_{te}) was calculated from the induced ΔV_{te} . The equivalent short circuit current (I_{sc}) was calculated from V_{te} and R_{te} according to Ohm's law. Another set of experiments was performed essentially as described previously (27). Briefly, a tissue area of 0.28 cm² was mounted in a conventional Ussing chamber filled with bicarbonate-

buffered Ringer's solution and gassed with 5% CO₂. Secretion was stimulated by apical addition of 1 μM forskolin. V_{te} and R_{te} were measured as above by applying $\pm 50 \mu\text{A}$ current pulses under open circuit conditions, and I_{sc} was calculated. By convention, a lumen-negative V_{te} corresponds to a positive short circuit current, which may be due to electrogenic cation absorption or anion secretion or a combination of both. An unpaired Student's *t* test was used to evaluate statistical significance. $p < 0.05$ was considered significant.

Histology—Mice were fixed by perfusion through the heart for 3–5 min with 4% paraformaldehyde in phosphate-buffered saline. For cryosections, organs were immersed in 10, 20, and 30% sucrose, embedded in Tissue-Tec, frozen, and sectioned at 8 or 10 μm . For Mayer's hematoxylin and eosin staining, tissues were dehydrated with isopropanol, embedded in paraffin, and sectioned at 5–8 μm . For staining, sections were deparaffinized using xylol and made hydrophilic by immersion in ethanol/water mixtures of decreasing ethanol content, and then stained and embedded in DPX resin (Merck) after water removal in the opposite order. Sections were visualized using the transmission mode of a Leica TCS2 confocal microscope or a Zeiss upright microscope equipped with a color CCD camera.

Real Time PCR—Mouse distal colon total RNA was prepared using Trizol (Invitrogen). RNA was subjected to DNase I digestion and purified with RNeasy (Qiagen) columns. cDNA was transcribed from 5 μg of total RNA with superscript II reverse transcriptase (Invitrogen) and random hexamers. The cDNA was diluted 1:25 for PCR in the presence of SYBR green. PCR was carried out on an AbiPrism 7900HT thermocycler (Applied Biosystems, California). Primers were selected to amplify 100–120-bp fragments across exon-exon boundaries. The following pairs were used: CFTR forward (5'-CAACCCTACATCTTCTAGCAA-CG-3') and CFTR reverse (5'-CAGATTCCAGTTGTTTGAGCTGC-3'); KCNQ1 forward (5'-CAAAGACCGTGGCAGTAACACC-3') and KCNQ1 reverse (5'-GGAGCATGTCTGTGATGATCACC-3'); and NKCC1 forward (5'-AACCAGAGATGCTGTGGTGC-3') and NKCC1 reverse (5'-CCCAATGTTTAAACATGCAGCG-3'). Three littermates were used for each genotype, and cDNA abundance was determined as the mean cycle at which the same predefined SYBR green signal was reached in each sample. Results are given as mean \pm S.E.

RESULTS

To investigate whether the disruption of both CFTR and CIC-2 leads to a more severe phenotype than a disruption of CFTR alone, we crossed CIC-2 knock-out mice (24) with two

TABLE I
Breeding results from doubly heterozygous parents compared to Mendelian predictions

		A. <i>Cfr</i> ^{+/-} / <i>Cln2</i> ^{+/-}		
CFTR	CIC-2	Obtained no.	Expected no.	Expected fraction
+/+	+/+	11	14	1/16
+/+	-/-	12	14	1/16
+/+	+/-	28	29	1/8
+/+	+/+	28	29	1/8
+/-	+/-	79	58	1/4
+/-	-/-	34	29	1/8
-/-	+/-	23	29	1/8
-/-	+/+	9	14	1/16
-/-	-/-	7	14	1/16
		B. <i>Cfr</i> ^{+/ΔF} / <i>Cln2</i> ^{+/-}		
CFTR	CIC-2	Obtained no.	Expected no.	Expected fraction
+/+	+/+	7	9	1/16
+/+	-/-	14	9	1/16
+/+	+/-	17	18	1/8
+/ ΔF	+/+	12	18	1/8
+/ ΔF	+/-	43	35	1/4
+/ ΔF	-/-	19	18	1/8
$\Delta\text{F}/\Delta\text{F}$	+/-	11	18	1/8
$\Delta\text{F}/\Delta\text{F}$	+/+	5	9	1/16
$\Delta\text{F}/\Delta\text{F}$	-/-	14	9	1/16

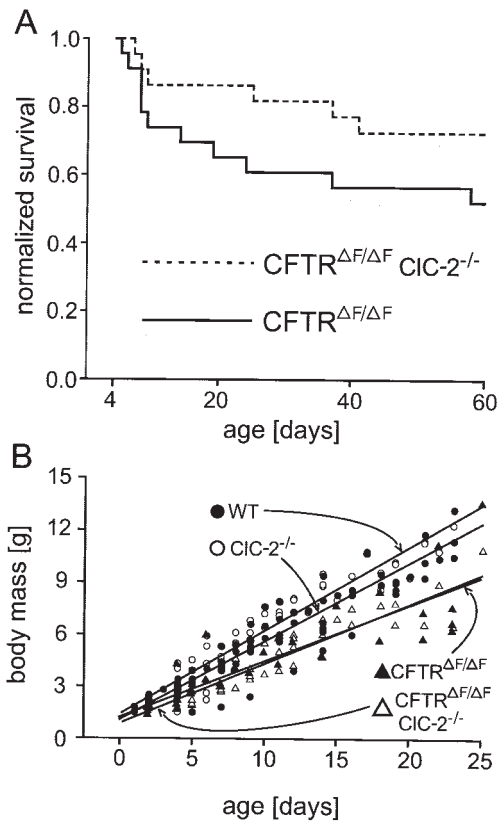


FIG. 1. Survival of *Cfr*^{ΔF/ΔF} and *Clcn2*⁻¹/*Cfr*^{ΔF/ΔF} mice (A) and weight development (B). A, a group of 23 *Cfr*^{ΔF/ΔF} mice (solid line) was compared with a group of 22 *Clcn2*⁻¹/*Cfr*^{ΔF/ΔF} double mutant mice (dashed line). The number of surviving mice was normalized to those living at day 4, when genotyping had been completed. Lethality was highest during the first week after birth. The Kolmogorov-Smirnov test revealed a significantly better survival rate for double mutant mice over *Cfr*^{ΔF/ΔF} mice on a $p < 0.05$ basis. B, weight development of WT, *Clcn2*⁻¹, *Cfr*^{ΔF/ΔF} and *Clcn2*⁻¹/*Cfr*^{ΔF/ΔF} mice. Weights were fitted with a linear function that described the data sufficiently well up to 25 days. Weight development was nearly identical in WT and *Clcn2*⁻¹ mice and in *Cfr*^{ΔF/ΔF} and *Clcn2*⁻¹/*Cfr*^{ΔF/ΔF} mice, respectively. $n > 5$ for each group.

different CFTR mouse models, *Cfr*^{ΔF/ΔF} (6) and *Cfr*⁻¹ (5). Both mice displayed a severe intestinal phenotype that led to occasional intestinal occlusion independent of the CIC-2 genotype. Moribund mice showed decreased food intake, signs of abdominal distress, and weight loss. When an autopsy was performed on such animals, it invariably revealed intestinal obstruction ($n = 9$).

The lethality of double mutant offspring from *Clcn2*⁺¹/*Cfr*^{+1/ΔF} or *Clcn2*⁺¹/*Cfr*⁺¹ double heterozygous matings was highest in the first week after birth, but some of these mice survived for >6 months (5 of 13 and 3 of 7 animals, respectively). The genotypes of offspring from these matings were determined in mice that had survived until tail biopsies were taken at day 3 ± 1 after birth and conformed roughly to Mendelian inheritance (Table I, A and B). Surprisingly, *Cfr*^{ΔF/ΔF}/*Clcn2*⁻¹ mice survived better than *Cfr*^{ΔF/ΔF} mice (Fig. 1). This difference, significant at a level of $p < 0.05$, was consistent with an apparent deviation from Mendelian inheritance of the number of mice that survived 3 ± 1 days after birth and resulted in a larger than expected number of *Cfr*^{ΔF/ΔF}/*Clcn2*⁻¹ animals (Table I, A and B). Unfortunately, attempts to perform a similar analysis with the *Cfr*⁻¹ line did not yield meaningful results because of poor breeding and high perinatal mortality. Weight development of *Cfr*^{ΔF/ΔF}/*Clcn2*⁻¹ double mutant mice was indistinguishable from that of

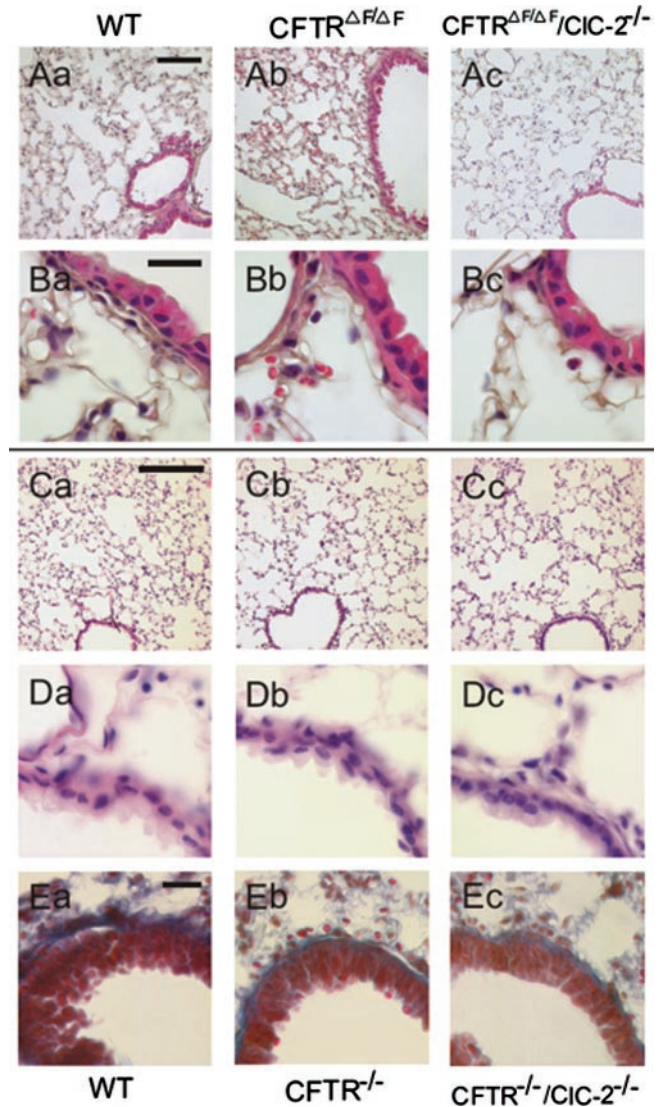


FIG. 2. Histological analysis of lung tissue from different genotypes. Paraffin sections from WT (left column; Aa–Ea), *Cfr*^{ΔF/ΔF} (center column; Ab and Bb), *Clcn2*⁻¹/*Cfr*^{ΔF/ΔF} (right column; Ac and Bc), *Cfr*⁻¹ (center column; Cb, Db, and Eb), and *Clcn2*⁻¹/*Cfr*⁻¹ mice (right column; Cc, Dc, and Ec) are shown. Aa–Ac and Ba–Bc are from age-matched, 1-year-old mice, Ca–Cc and Da–Dc are from 8-month-old mice, and all were stained with hematoxylin and eosin. The bronchus walls are shown in higher magnification in Ba–Bc and Da–Dc. Ea–Ec are sections from 2-month-old litter mates and were stained with azan. Azan is a mixture of azocarmine, orange G, and aniline blue, the latter of which stains fibrotic tissue, in particular collagen, with an intensive blue. The scale bar in Aa represents 100 μm for Aa–Ac, the bar in Ba represents 20 μm for Ba–Bc, the bar in Ca represents 80 μm for Ca–Cc and 12.5 μm for Da–Dc, and the bar in Ea represents 20 μm for Ea–Ec. Neither fibrosis nor inflammation was observed.

Cfr^{ΔF/ΔF} mice and lagged behind the weight development of WT and *Clcn2*⁻¹ mice (Fig. 1B).

CFTR mouse models suffer from intestinal occlusion (26), but, in contrast to human patients, the mice rarely develop lung or pancreatic phenotypes. We therefore investigated whether the additional disruption of the CIC-2 Cl⁻ channel led to morphological changes in these and other tissues. Comparative histological analysis was performed at 1, 2, 3, 8, and 12 months of age.

Lung sections of 2, 8, and 12-month-old mice were stained with hematoxylin and eosin (staining nucleic acids and proteins, respectively) or with azan, which stains fibrotic tissue in blue (Fig. 2). No difference in lung morphology could be detected between age-matched wild type (Fig. 2, Aa and Ba),

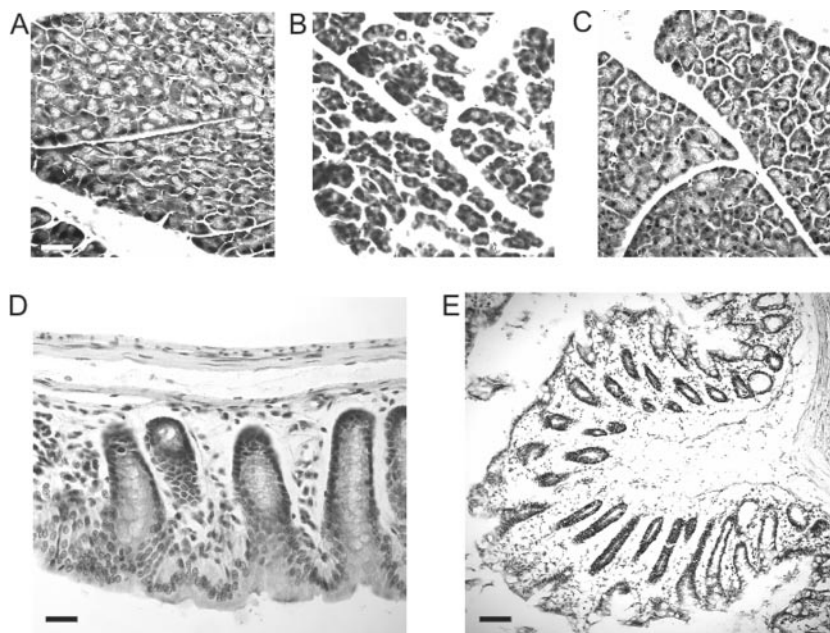


FIG. 3. Pancreas and colon morphology of WT, *Cfr*^{-/-}, and *Cfr*^{-/-}/*Clcn2*^{-/-} mice. A–C, pancreatic sections from 8-month-old WT (A), *Cfr*^{-/-} (B), and *Cfr*^{-/-}/*Clcn2*^{-/-} (C) mice. Note the absence of fibrotic or cystic changes. D and E, colon section from *Cfr*^{-/-}/*Clcn2*^{-/-} mice aged 8 months (D) and one year (E) with no signs of abdominal distress prior to analysis. There were no abnormalities. All sections were stained with hematoxylin and eosin. The scale bar in A represents 20 μm for A–C, the bar in D represents 20 μm , and the bar in E represents 100 μm .

Cfr ^{$\Delta\text{F}/\Delta\text{F}$} (Fig. 2, *Ab* and *Bb*), and *Clcn2*^{-/-}/*Cfr* ^{$\Delta\text{F}/\Delta\text{F}$} (Fig. 2, *Ac* and *Bc*) mice, or between litter mate wild type (Fig. 2, *Ca*, *Da*, and *Ea*), *Cfr*^{-/-} (*Cb*, *Db*, and *Eb*), and *Clcn2*^{-/-}/*Cfr*^{-/-} (*Cc*, *Dc*, and *Ec*) mice. In particular, there was no evidence for inflammatory infiltration or fibrosis. Even in 1-year-old *Clcn2*^{-/-}/*Cfr* ^{$\Delta\text{F}/\Delta\text{F}$} mice there was no evidence for morphological lung abnormalities (Fig. 2, *Ac* and *Bc*).

Histological analysis of the pancreas (Fig. 3, A–C) from WT (Fig. 3A), *Cfr*^{-/-} (Fig. 3B), and *Clcn2*^{-/-}/*Cfr*^{-/-} animals (Fig. 3C) did not reveal differences up to an age of 8 months either. Specifically, the pancreas lacked the signs of fibrosis, cystic changes, or inflammation that are seen in human CF. Likewise, the colon of *Clcn2*^{-/-}/*Cfr*^{-/-} mice (Fig. 3, D and E) was unremarkable up to 8 months, when mice free of abdominal distress were investigated. The epithelium was normal, without inflammation or mucoid retention in goblet cells or at the base of the crypts. Similar results were obtained in the small intestine. The liver, including the bile duct epithelia, lacked pathological changes.

However, an impairment of physiological function is not necessarily paralleled by morphological alterations. We therefore performed Ussing chamber experiments to assess whether the additional disruption of CIC-2 exacerbated the defects in trans-epithelial chloride transport that are caused by CFTR mutations (Fig. 4). Ion transport across colonic epithelia has three main components, *i.e.* aldosterone-stimulated Na⁺ reabsorption, cAMP-stimulated Cl⁻ secretion, and K⁺ secretion. These processes involve luminal ENaC Na⁺ channels, luminal CFTR Cl⁻ channels, and luminal K⁺ channels not yet identified at the molecular level, respectively. Na⁺ reabsorption and Cl⁻ secretion result in positive *I*_{sc} components, whereas K⁺ secretion is manifested by a negative *I*_{sc} component. These different components can be dissected pharmacologically by using stimulatory and inhibitory drugs. To increase the sensitivity of detection for Cl⁻ currents, ENaC was blocked by adding 10 μM amiloride to the apical perfusate. In experiments on WT colon (Fig. 4A), the subsequent basolateral addition of 10 μM forskolin, an activator of adenylate cyclase, drastically increased *I*_{sc}. This positive current component is likely to represent cAMP-activated Cl⁻ secretion into the lumen via CFTR. This was indirectly confirmed by the inhibitory effect of the subsequent basolateral addition of 100 μM bumetanide, an inhibitor of Na⁺-K⁺-2Cl⁻ cotransport. The latter is responsible for the

cytoplasmic accumulation of Cl⁻ as a prerequisite for a chloride secretory response (see Fig. 6 for transport model). In the experiments of Fig. 4, B and C, which show typical recordings for the *Cfr* ^{$\Delta\text{F}/\Delta\text{F}$} and the *Clcn2*^{-/-}/*Cfr* ^{$\Delta\text{F}/\Delta\text{F}$} colon, respectively, the positive forskolin-induced *I*_{sc} component was missing, which is consistent with the absence of an apical cAMP-stimulated CFTR chloride channel. In the absence of functional CFTR, forskolin induced a negative *I*_{sc} component. There was no statistically significant difference in forskolin-stimulated currents between the wild-type and the *Clcn2*^{-/-} colon irrespective of the CFTR genotype (WT or *Cfr* ^{$\Delta\text{F}/\Delta\text{F}$}) (Fig. 4D).

The negative current component observed under amiloride and forskolin in CFTR mutant mice cannot be due to a stimulation of Cl⁻ secretion or a stimulation of cation reabsorption. Experiments using 5 mM Ba²⁺, an inhibitor of certain classes of K⁺ channels, revealed that this negative *I*_{sc} component can be explained by K⁺ secretion. Ba²⁺ caused a significant inhibition only from the luminal but not from the basolateral side, which is consistent with a specific effect on luminal K⁺ channels (Fig. 4B).

Thus, genetic ablation of CFTR function essentially abolished cAMP-dependent Cl⁻ secretion and unmasked a cAMP-stimulated K⁺ secretion. Both the basolateral KCNQ1/KCNE3 K⁺ channels (28) and the NKCC1 cotransporter (29) (Fig. 6) are activated by cAMP. This may explain the prominent secretion of K⁺ during stimulation with cAMP, although we cannot rule out a direct effect on apical K⁺ channels. In the Ussing chamber experiments described so far, colonic epithelia from *Cfr* ^{$\Delta\text{F}/\Delta\text{F}$} /*Clcn2*^{-/-} (Fig. 4C) behaved similarly to tissues in which only CFTR has been mutated (Fig. 4B), as was evaluated statistically in Fig 4D.

Although there was no obvious influence of CIC-2 on the short circuit current under stimulation in the experiments described so far, we performed additional experiments under more physiological conditions to further investigate this issue. A bicarbonate-buffered bath solution and lower concentrations of forskolin (1 μM instead of 10 μM) were used. These conditions may lead to less than maximal CFTR activation, thereby facilitating the detection of the relative contribution of CIC-2 to anion secretion. We also used mice that were kept on low sodium diet, a procedure known to up-regulate apical ENaC, thus allowing us to test the viability of the tissue. In Ussing chamber experiments, currents across *Clcn2*^{+/-} control and

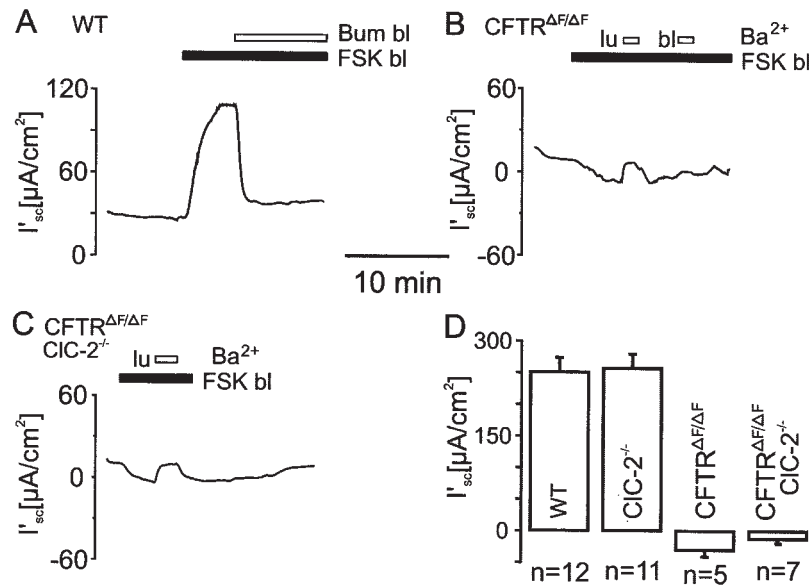


FIG. 4. Transepithelial current across colonic epithelia as determined by Ussing chamber experiments. Equivalent short circuit current (I_{sc}) traces for WT (A), $Cftr^{\Delta F/\Delta F}$ (B), and $Cftr^{\Delta F/\Delta F}/Cln2^{-/-}$ colon (C) are shown. Amiloride ($10 \mu M$), present throughout all the registrations shown in A–C, was used to block Na^+ currents through ENaC, forskolin (FSK; $10 \mu M$) was used to raise cAMP by stimulating adenylate cyclase, bumetanide (Bum; $100 \mu M$) was used to inhibit $Na^+-K^+-2Cl^-$ cotransport, and $5 mM Ba^{2+}$ was used to inhibit certain K^+ channels. The application was either from the luminal (lu) or basolateral (bl) side. D, averaged I_{sc} after forskolin stimulation in the presence of amiloride. The n for each group is given at the bottom of D, and the error bars represent S.E. Forskolin increased I_{sc} from $30.0 \pm 7.6 \mu A/cm^2$ to $255.0 \pm 26.5 \mu A/cm^2$ in WT ($n = 12$), and from 76.5 ± 11.3 to $257.1 \pm 22.2 \mu A/cm^2$ in $Cln2^{-/-}$ colon ($n = 11$). In $Cftr^{\Delta F/\Delta F}$ colon, forskolin changed I_{sc} from a baseline current of -15.9 ± 15.7 to $-30.5 \pm 10.7 \mu A/cm^2$ ($n = 5$), and in $Cln2^{-/-}/Cftr^{\Delta F/\Delta F}$ colon the baseline current was changed from 9.3 ± 7.1 to $-12.8 \pm 7 \mu A/cm^2$ ($n = 7$).

$Cln2^{-/-}$ colonic tissue were compared (Fig. 5, A and B, respectively). The inhibitory effect of apical amiloride revealed that almost all resting I_{sc} was due to Na^+ reabsorption through ENaC. In the continued presence of amiloride, the application of $1 \mu M$ forskolin to the apical bath elicited a positive I_{sc} component. This result was due to anion secretion, as revealed by the inhibition of this current component with the luminal addition of the chloride channel inhibitor DPC ($1 mM$) at the end of the experiment. Application of luminal Ba^{2+} resulted in a small additional increase in I_{sc} in both control and $Cln2^{-/-}$ mice, revealing, as in Fig. 4, B and C, a K^+ -secretory component. This component was minor in comparison with the large anion secretory I_{sc} component. A statistical evaluation of the I_{sc} values is given in Fig. 5C. There was no significant influence of the $Cln2$ genotype on the Na^+ current (Fig. 5C, first two columns on the left). However, forskolin-induced anion secretory currents were roughly 40% larger in $Cln2^{-/-}$ mice than in $Cln2^{+/+}$ mice ($p < 0.001$) (Fig. 5C). This result is surprising, as it is incompatible with the postulated secretory role of apical CIC-2 channels in colonic epithelia. One might argue, however, that CFTR may be up-regulated in response to the absence of CIC-2. To address this issue, CFTR mRNA abundance in the WT and $Cln2^{-/-}$ colons of three littermate pairs was compared by real-time PCR. The K^+ channel, KCNQ1, and the $Na^+/K^+/2Cl^-$ cotransporter, NKCC1, both of which are expressed in colonic epithelia (28), were used as controls. As shown in Table II, there was no significant difference in transcript levels. This, however, does not strictly exclude a difference in the number of active CFTR channels.

Because both CFTR and CIC-2 are also expressed in the heart (15), electrocardiogram recordings were performed on anesthetized $Cftr^{-/-}$, $Cln2^{-/-}$, and $Cln2^{-/-}/Cftr^{-/-}$ mice. No arrhythmia or other abnormalities were detected ($n = 2$ for each genotype; data not shown).

DISCUSSION

Several regulatory functions have been proposed for CFTR, the gene product affected in cystic fibrosis (31). However, its

main role is in salt and fluid transport, where it serves as a cAMP-activated Cl^- channel in the apical membrane of several epithelia. In the colon and in pancreatic ducts, CFTR mediates Cl^- secretion, but the direction of Cl^- transport in lung epithelia is controversial (32). These three tissues are the main sites of pathological changes in cystic fibrosis. In addition, CFTR is also expressed in several other tissues such as the kidney and the heart, where its function is less clear.

The chloride channels that are expressed in the same epithelial membranes as CFTR are interesting in regard to cystic fibrosis for two reasons. First, the genetic variability in their expression levels or functional properties may influence the severity of cystic fibrosis, as these channels will co-determine the extent of remaining Cl^- transport in the absence of functional CFTR. Thus, genes encoding such chloride channels may be modifier genes for cystic fibrosis (7, 8). A differential expression in mice and men might explain the fact that CFTR knock-out mice do not exhibit the full CF phenotype observed in humans. Second, such channels are potentially interesting targets for pharmacological intervention. Specific openers of these channels might be useful in treating CF.

CIC-2 is almost ubiquitously expressed (15) and is therefore present in the airway, colonic, and pancreatic epithelia, whose function is compromised in cystic fibrosis. Furthermore, several studies suggested that CIC-2 may be present in apical membranes of lung (18) and intestinal (19, 33) epithelia, although others obtained conflicting results (34, 35). Finally, the testicular and retinal degeneration observed in $Cln2^{-/-}$ mice was suggested to result from a defect in transepithelial transport across the Sertoli cell and retinal pigment epithelium, respectively (24).

Thus, CIC-2 appeared to be an excellent candidate for a chloride channel that operates in parallel to CFTR and may modulate the CF phenotype. To finally clarify this issue, which has been raised in several reports (21–23), we mated $Cln2^{-/-}$ mice (24) with CFTR mouse models. We used a line, $Cftr^{-/-}$ (5), which results in a complete loss of CFTR function, as well as

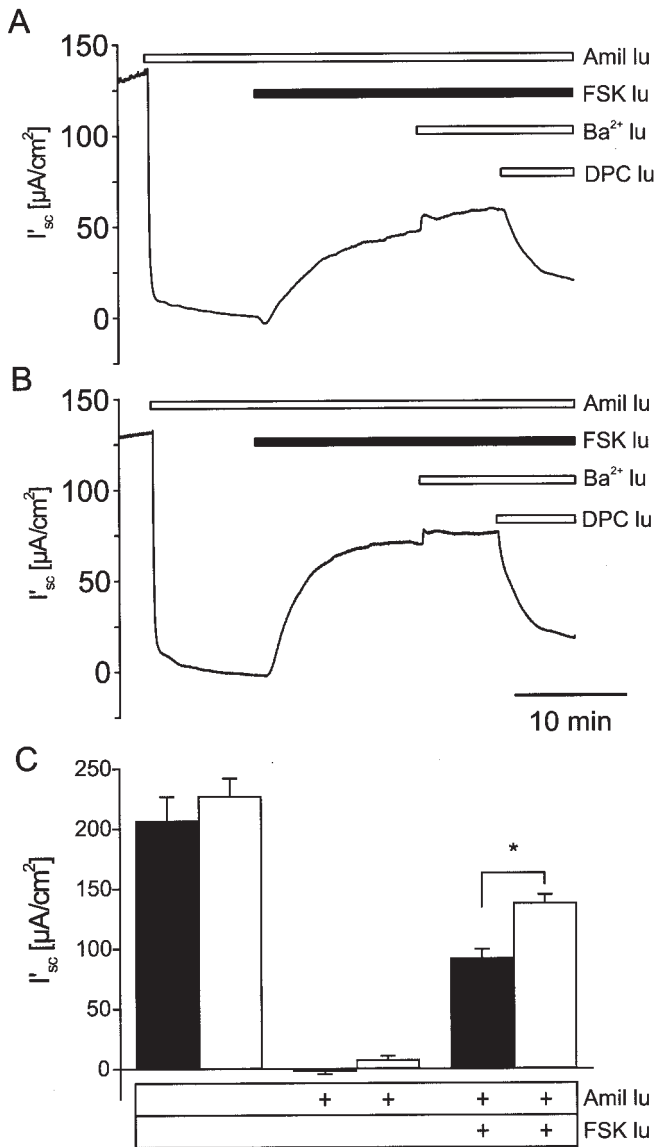


FIG. 5. Comparison of transepithelial current in distal colon from control, *Clcn2*^{+/-} (A), and *Clcn2*^{-/-} mice (B). In contrast to the experiments in Fig. 4, mice had been kept on low sodium diet. This led to a significant positive I_{sc} component due to Na^+ absorption from the lumen that could be blocked by the ENaC inhibitor amiloride (10 μM). In addition, a lower concentration of forskolin (1 μM) was used. In the presence of functional CFTR, luminal Ba^{2+} only marginally changed short circuit current, which was strongly inhibited by the CFTR inhibitor DPC. In C, the data from *Clcn2*^{+/-} ($n = 30$) (black bars) and *Clcn2*^{-/-} ($n = 33$) (white bars) were compared. The difference between I_{sc} in the presence of amiloride and forskolin was significant at the $p = 0.001$ level.

Cftr ^{$\Delta\text{F}/\Delta\text{F}$} mice (6), which carry an in-frame deletion of phenylalanine 508. The latter mice survived longer and therefore allowed us to assess the effect of an additional disruption of *Clcn2* in older animals. The deletion of Phe-508 ($\Delta\text{F}508$), which is the most common CFTR mutation in Caucasian CF patients, results in a temperature-sensitive trafficking defect in an otherwise functional CFTR Cl^- channel to the cell surface (36).

Contrary to what might have been expected, the additional disruption of the CIC-2 channel was neither lethal nor did it result in a higher mortality. In our study, *Cftr* ^{$\Delta\text{F}/\Delta\text{F}$} /*Clcn2*^{-/-} mice survived better than *Cftr* ^{$\Delta\text{F}/\Delta\text{F}$} mice. Morphological changes could not be detected in double mutant mouse tissues (lung, pancreas, and colon) that are affected in human CF patients, even when long-time surviving animals were investi-

TABLE II

Quantitative reverse transcription PCR on distal colon RNA

Mean cycle \pm S.E. Two different primer pairs for each transcript were used on cDNA transcribed from three different, age-matched WT and *Clcn2*^{-/-} mice.

	Wild type colon	<i>Clcn2</i> ^{-/-} colon
CFTR	30.83 \pm 0.29	31.02 \pm 0.32
KCNQ1	36.06 \pm 0.39	36.60 \pm 0.21
NKCC1	30.42 \pm 0.17	30.66 \pm 0.12

gated. The inflammatory infiltrates and goblet cell hyperplasia reported to be present occasionally in CFTR mouse colon (26) were not detected in our study. These phenotypes may not have developed because our mice were kept on an oral laxative in a good hygienic and nutritional state. As CIC-2 is expressed in the lung earlier than CFTR, it was postulated to mediate the chloride fluxes deemed to be important for lung development (37). We have shown previously that CIC-2 is not necessary for lung development (24). This work shows that, even in a CFTR-deficient background, lung morphology is normal. A recent paper has again raised this issue using CIC-2 antisense oligonucleotides (38). However, oligonucleotides with identical sequences were used in a study on choroid plexus chloride channels (39), and they later turned out to down-regulate a chloride channel not related to CIC-2 (40). The lack of an overt pulmonary CF-like phenotype in *Cftr*^{-/-} mice may also be due to differences in mouse and human lung morphology (41).

Ussing chamber experiments on colon epithelia confirmed the well known impairment of cAMP-stimulated anion current in CF for two CFTR mouse models. The finding that the additional disruption of CIC-2 did not lead to less colonic anion secretion does not support the hypothesis that CIC-2 provides a significant anion current in parallel to that mediated by CFTR. Hence, CIC-2 is unlikely to mitigate the pathophysiological effects in cystic fibrosis. However, these results do not strictly rule out the possibility that CIC-2 may be expressed in the apical membranes that also express CFTR, although it does not mediate significant currents under our experimental conditions.

A different subcellular localization is suggested by the better survival of *Clcn2*^{-/-}/*Cftr* ^{$\Delta\text{F}/\Delta\text{F}$} as compared with *Cftr* ^{$\Delta\text{F}/\Delta\text{F}$} mice and the second set of Ussing chamber experiments on colonic tissues. When comparing currents from *Clcn2*^{-/-} and *Clcn2*^{+/-} (control) mice during moderate apical stimulation with 1 μM forskolin in the presence of physiological bicarbonate concentrations, cAMP-activated currents were actually increased in mice lacking CIC-2. A less than maximal stimulation of apical CFTR may render the detection of the contribution of Cl^- currents mediated by CIC-2 more sensitive, and the presence of bicarbonate, which can permeate through CFTR (42), may modulate several conductances via changes in pH_i . We do not know which of these factors accounts for the fact that we detected a difference in anion secretion between WT and *Clcn2*^{-/-} mice under these conditions but not under the conditions of the experiments shown in Fig. 4. The increase in anion secretion observed in the CIC-2 knock-out could not be accounted for by an up-regulation of CFTR message. It might instead be explained by a basolateral rather than an apical localization of CIC-2, as depicted in the model of Fig. 6. Any additional anion conductance in the same (apical) membrane as CFTR should increase transepithelial anion secretion, whereas a basolateral chloride efflux would lower the intracellular anion concentration and decrease apical anion exit. Basolateral Cl^- -channels would also depolarize the basolateral voltage toward E_{Cl} , thereby decreasing V_{te} and, hence, the short circuit current. With such a localization, CIC-2 disruption should result in an enhanced anion secretion.

In fact, the subcellular localization of CIC-2 in colonic epi-

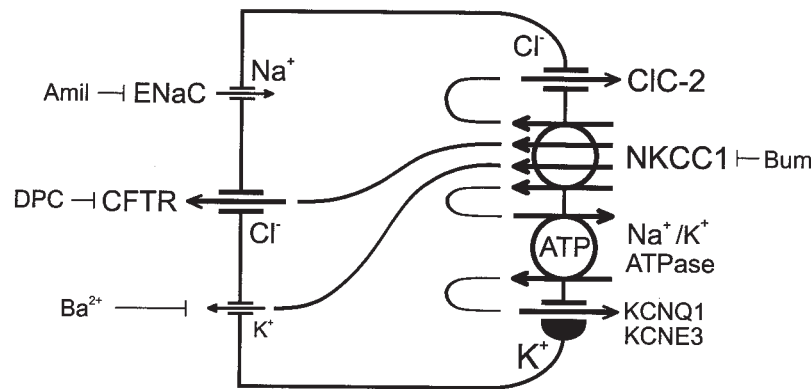


FIG. 6. Model for transepithelial transport in the colon. The Na^+ gradient generated by the basolateral $3\text{Na}^+-2\text{K}^+$ ATPase is used by the basolateral $\text{Na}^+-\text{K}^+-2\text{Cl}^-$ cotransporter NKCC1 to accumulate intracellular Cl^- above its electrochemical equilibrium. This requires a basolateral K^+ conductance for K^+ recycling that is predominantly mediated by the KCNQ1/KCNE3 K^+ channels that hyperpolarize the basolateral membrane. A minor fraction of K^+ leaves the cell through apical Ba^{2+} -inhibitable K^+ channels. Cl^- leaves the cell apically through DPC-inhibitable CFTR Cl^- channels. Apical CFTR Cl^- channels, basolateral KCNQ1/KCNE1 K^+ channels, and NKCC1 co-transporters are all stimulated by cAMP (not shown). The apical membrane also contains the Na^+ channel ENaC, which is up-regulated by aldosterone and mediates Na^+ reabsorption.

thelia is controversial. On the one hand, antibodies against CIC-2 detected signals in apical membranes of intestinal membranes in a study by Zeitlin and co-workers (33), whereas Bear and co-workers (19), using a different CIC-2 antiserum, found immunoreactivity predominantly at the apical junctional complexes of murine intestinal epithelia. By contrast, a third antiserum by Lipecka, Fritsch and co-workers (34) stained the basolateral membranes of rat small intestine and colon. Finally, Catalán, Cid and coworkers (35), using a commercial anti-CIC-2 antibody (Alomone), found basolateral staining of guinea pig colonocytes. None of these studies included controls with knock-out tissues, raising the possibility that some of these results may reflect nonspecific binding. Our own antibody (24) is not suited for immunocytochemistry in most tissues. Experiments using *Cln2*^{-/-} mice as control showed that the Alomone serum was not useful (24). Thus, the proposed apical localization of CIC-2 in epithelia affected by CF should be viewed with considerable caution. Carefully controlled immunohistochemical studies, which probably require better antibodies, are desirable to clarify this issue.

A basolateral localization of CIC-2, as suggested indirectly by our Ussing chamber experiments, might also explain the observation that *Cftr*^{ΔF/ΔF} mice survived better when CIC-2 was additionally disrupted. The small amount of functional CFTR that remains in the apical membranes of *Cftr*^{ΔF/ΔF} colonocytes might mediate more anion secretion in the absence of CIC-2 (Fig. 6). In Ussing chamber experiments these small currents will be swamped by larger K^+ secretory currents elicited by forskolin and, hence, are difficult to detect (Fig. 4D).

We also recorded electrocardiograms, as both CFTR (43) and CIC-2 (15) are expressed in the heart. The possible function of either channel in cardiac myocytes is unclear, and there are no obvious cardiac abnormalities in patients with cystic fibrosis. Although it was hypothesized that CIC-2 might have an important function in the heart (44), we could not detect any ECG abnormalities even in animals that lacked both Cl^- channels. This does not rule out infrequent episodes of arrhythmia, which may have escaped our analysis.

In conclusion, CIC-2 disruption does not worsen the pathogenic effects of CFTR disruption in mice. Neither did the additional disruption of CIC-2 lead to histopathological changes in tissues that are severely affected in cystic fibrosis patients but are spared in CFTR knock-out mice. A basolateral localization of CIC-2, as suggested indirectly by the present results, needs to be confirmed by immunocytochemistry once better antibodies are available. Such localization would predict that inhibi-

tion rather than activation of CIC-2 should mitigate the phenotype resulting from CFTR mutations that do not abolish its currents completely.

Acknowledgments—We thank Mirja Laschet for technical assistance and Dr. Olaf Scheel for help with PERL scripts.

REFERENCES

- Riordan, J. R., Rommens, J. M., Kerem, B., Alon, N., Rozmahel, R., Grzelczak, Z., Zielenski, J., Lok, S., Plavsic, N., Chou, J. L., Drumm, M. L., Iannuzzi, M. C., Collins, F. S., and Tsui, L.-C. (1989) *Science* **245**, 1066–1073
- Stutts, M. J., Canessa, C. M., Olsen, J. C., Hamrick, M., Cohn, J. A., Rossier, B. C., and Boucher, R. C. (1995) *Science* **269**, 847–850
- Schwiebert, E. M., Egan, M. E., Hwang, T. H., Fulmer, S. B., Allen, S. S., Cutting, G. R., and Guggino, W. B. (1995) *Cell* **81**, 1063–1073
- Kunzelmann, K., Mall, M., Briel, M., Hipper, A., Nitschke, R., Ricken, S., and Greger, R. (1997) *Pflügers Arch.* **435**, 178–181
- Snouwaert, J. N., Brigman, K. K., Latour, A. M., Malouf, N. N., Boucher, R. C., Smithies, O., and Koller, B. H. (1992) *Science* **257**, 1083–1088
- Zeiger, B. G., Eichwald, E., Zabner, J., Smith, J. J., Puga, A. P., McCray, P. B., Jr., Capecchi, M. R., Welsh, M. J., and Thomas, K. R. (1995) *J. Clin. Invest.* **96**, 2051–2064
- Gyömörey, K., Rozmahel, R., and Bear, C. E. (2000) *Pediatr. Res.* **48**, 731–734
- Rozmahel, R., Wilschanski, M., Matin, A., Plyte, S., Oliver, M., Auerbach, W., Moore, A., Forstner, J., Durie, P., Nadeau, J., Bear, C., and Tsui, L. C. (1996) *Nat. Genet.* **12**, 280–287
- Jentsch, T. J., Stein, V., Weinreich, F., and Zdebek, A. A. (2002) *Physiol. Rev.* **82**, 503–568
- Koch, M. C., Steinmeyer, K., Lorenz, C., Ricker, K., Wolf, F., Otto, M., Zoll, B., Lehmann-Horn, F., Grzeschik, K. H., and Jentsch, T. J. (1992) *Science* **257**, 797–800
- Simon, D. B., Bindra, R. S., Mansfield, T. A., Nelson-Williams, C., Mendonca, E., Stone, R., Schurman, S., Nayir, A., Alpay, H., Bakkaloglu, A., Rodriguez-Soriano, J., Morales, J. M., Sanjad, S. A., Taylor, C. M., Pilz, D., Brem, A., Trachtman, H., Griswold, W., Richard, G. A., John, E., and Lifton, R. P. (1997) *Nat. Genet.* **17**, 171–178
- Lloyd, S. E., Pearce, S. H., Fisher, S. E., Steinmeyer, K., Schwappach, B., Scheinman, S. J., Harding, B., Bolino, A., Devoto, M., Goodyer, P., Rigden, S. P., Wrong, O., Jentsch, T. J., Craig, I. W., and Thakker, R. V. (1996) *Nature* **379**, 445–449
- Kornak, U., Kasper, D., Bosl, M. R., Kaiser, E., Schweizer, M., Schulz, A., Friedrich, W., Dellling, G., and Jentsch, T. J. (2001) *Cell* **104**, 205–215
- Haug, K., Warnstedt, M., Alekov, A. K., Sander, T., Ramirez, A., Poser, B., Maljevic, S., Hebeisen, S., Kubisch, C., Rebstock, J., Horvath, S., Hallmann, K., Dullinger, J. S., Rau, B., Haverkamp, F., Beyenburg, S., Schulz, H., Janz, D., Giese, B., Müller-Newen, G., Propping, P., Elger, C. E., Fahlke, C., Lerche, H., and Heils, A. (2003) *Nat. Genet.* **33**, 527–532
- Thiemann, A., Grunder, S., Pusch, M., and Jentsch, T. J. (1992) *Nature* **356**, 57–60
- Steinmeyer, K., Ortlund, C., and Jentsch, T. J. (1991) *Nature* **354**, 301–304
- Estévez, R., Boettger, T., Stein, V., Birkenhäger, R., Otto, E., Hildebrandt, F., and Jentsch, T. J. (2001) *Nature* **414**, 558–561
- Murray, C. B., Morales, M. M., Flotte, T. R., McGrath-Morrow, S. A., Guggino, W. B., and Zeitlin, P. L. (1995) *Am. J. Respir. Cell Mol. Biol.* **12**, 597–604
- Gyömörey, K., Yeager, H., Ackerley, C., Garami, E., and Bear, C. E. (2000) *Am. J. Physiol.* **279**, C1787–C1794
- Jordt, S. E., and Jentsch, T. J. (1997) *EMBO J.* **16**, 1582–1592
- Schwiebert, E. M., Cid-Soto, L. P., Stafford, D., Carter, M., Blaisdell, C. J., Zeitlin, P. L., Guggino, W. B., and Cutting, G. R. (1998) *Proc. Natl. Acad. Sci. U. S. A.* **95**, 3879–3884
- Blaisdell, C. J., Edmonds, R. D., Wang, X. T., Guggino, S., and Zeitlin, P. L. (2000) *Am. J. Physiol.* **278**, L1248–L1255

23. Gründer, S., Thiemann, A., Pusch, M., and Jentsch, T. J. (1992) *Nature* **360**, 759–762
24. Bösl, M. R., Stein, V., Hübner, C., Zdebik, A. A., Jordt, S. E., Mukhopadhyay, A. K., Davidoff, M. S., Holstein, A. F., and Jentsch, T. J. (2001) *EMBO J.* **20**, 1289–1299
25. Nehrke, K., Arreola, J., Nguyen, H. V., Pilato, J., Richardson, L., Okunade, G., Baggs, R., Shull, G. E., and Melvin, J. E. (2002) *J. Biol. Chem.* **277**, 23604–23611
26. Grubb, B. R., and Boucher, R. C. (1999) *Physiol. Rev.* **79**, S193–S214
27. Cuffe, J. E., Bertog, M., Velazquez-Rocha, S., Dery, O., Bunnett, N., and Korbmayer, C. (2002) *J. Physiol.* **539**, 209–222
28. Schroeder, B. C., Waldegger, S., Fehr, S., Bleich, M., Warth, R., Greger, R., and Jentsch, T. J. (2000) *Nature* **403**, 196–199
29. Tanimura, A., Kurihara, K., Reshkin, S. J., and Turner, R. J. (1995) *J. Biol. Chem.* **270**, 25252–25258
30. Deleted in proof
31. Kunzelmann, K. (2001) *News Physiol. Sci.* **16**, 167–170
32. Guggino, W. B. (1999) *Cell* **96**, 607–610
33. Murray, C. B., Chu, S., and Zeitlin, P. L. (1996) *Am. J. Physiol.* **271**, L829–L837
34. Lipecka, J., Bali, M., Thomas, A., Fanen, P., Edelman, A., and Fritsch, J. (2002) *Am. J. Physiol.* **282**, C805–C816
35. Catalán, M., Cornejo, I., Figueroa, C. D., Niemeyer, M. I., Sepúlveda, F. V., and Cid, L. P. (2002) *Am. J. Physiol.* **283**, G1004–G1013
36. French, P. J., van Doorninck, J. H., Peters, R. H., Verbeek, E., Ameen, N. A., Marino, C. R., de Jonge, H. R., Bijman, J., and Scholte, B. J. (1996) *J. Clin. Invest.* **98**, 1304–1312
37. Chu, S., Blaisdell, C. J., Liu, M. Z., and Zeitlin, P. L. (1999) *Am. J. Physiol.* **276**, L614–L624
38. Blaisdell, C. J., Morales, M. M., Andrade, A. C., Bamford, P., Wasicko, M., and Welling, P. (2004) *Am. J. Physiol.* **286**, L420–L426
39. Kajita, H., Omori, K., and Matsuda, H. (2000) *J. Physiol.* **523**, 313–324
40. Speake, T., Kajita, H., Smith, C. P., and Brown, P. D. (2002) *J. Physiol.* **539**, 385–390
41. Verkman, A. S., Song, Y., and Thiagarajah, J. R. (2003) *Am. J. Physiol.* **284**, C2–C15
42. Poulsen, J. H., Fischer, H., Illek, B., and Machen, T. E. (1994) *Proc. Natl. Acad. Sci. U. S. A.* **91**, 5340–5344
43. Levesque, P. C., Hart, P. J., Hume, J. R., Kenyon, J. L., and Horowitz, B. (1992) *Circ. Res.* **71**, 1002–1007
44. Duan, D., Ye, L., Britton, F., Horowitz, B., and Hume, J. R. (2000) *Circ. Res.* **86**, E63–E71